Original Article | Journal of Biosystems Engineering

J. of Biosystems Eng. 37(2):113-121. (2012. 4)
http://dx.doi.org/10.5307/JBE.2012.37.2.113

eISSN : 2234-1862
pISSN : 1738-1266

Characteristics of Particle Separation in Suspension using an Ultrasonic Standing Wave

Beom-Soo Shin[1]*, Mary-Grace C. Danao[2]

[1]Dept. of Biosystems Engineering, Kangwon National University, Chuncheon, Korea, [2]Dept. of Agricultural and Biological Engineering, University of Illinois at Urbana-Champaign, Urbana, IL, U.S.A

Received: March 31th, 2012; Revised: April 24th, 2012; Accepted: April 26th, 2012

Abstract

Purpose: Particle separation in solution is one of important process in a unit operation as well as in an extract preparation for biosensors. Contrary to centrifuge-type of mesh-type filter, using an ultrasonic standing wave make the filtering process continuous and free from maintenance. It is needed to investigate the characteristics of particle movement in the ultrasonic standing wave field. **Methods:** Through the computer simulation the effects of major design and driving parameters on the alignment characteristics of particles were investigated, and a cylindrical chamber with up-stream flow type was devised using two circular-shape PZTs on both sides of the chamber, one for transmitting ultrasonic wave and the other for just reflecting it. Then, the system performance was experimentally investigated as well. **Results:** The speed of a particle to reach pressure-node plane increased as the acoustic pressure and size of particle increased. The maximum allowable up-stream flow rate could be calculated as well. As expected, exact numbers of pressure-node planes were well formed at specific locations according to the wavelength of ultrasonic wave. As the driving frequency of PZT got close to its resonance frequency, the bands of particles were observed clearer, which meant the particles were trapped into narrower space. Higher excitation voltages to the PZT produced a greater acoustic force with which to trap particles in the pressure-node planes, so that the particles gathered could move upwards without disturbing their alignments even at a higher inlet flow rate. **Conclusions:** This research showed the feasibility of particle separation in solution in the continuous way by an ultrasonic standing wave. Further study is needed to develop a device to collect or harvest those separated particles.

Keywords: USW (Ultrasonic Standing Wave), PZT, Cylindrical-type chamber, Microparticle, Separation

Introduction

An ultrasonic standing wave (USW) is defined as the condition when two waves with the same frequency progressed facing each other become overlapped, to give the effect as if the ultrasounds under progress are standing still in the field. An ultrasonic standing wave is generated by using two acoustic sources facing each other, or one acoustic source that is facing a reflector. The ultrasonic sources commonly used are piezo-ceramic elements; an ultrasonic standing wave generating device is constructed either by directly coupling this element into a liquid, or doing so via other coupling layers (Laurell et al., 2007). An ultrasonic wave is longitudinal, and particles in the field are made to move in a forward and backward direction, according to the direction of wave advance. Therefore, a one dimensional ultrasonic standing wave is formed when an appropriate gap between a transducer and reflector is maintained, so that the progressive wave and reflected wave can join at a suitable phase relation. At a certain point, anti-pressure node planes, which are vibrating inbetween ± maximum level from an equilibrium stage, are formed while pressure node planes are created of either the minimum level or 0 at locations 1/4 wavelength apart (Tolt and Feke, 1993). Particles which are relatively small as compared with the wavelength, when they are exposed to the ultrasonic standing wave, move to the

***Corresponding author:** Beom-Soo Shin
Tel: +82-33-250-6493; **Fax:** +82-33-255-6406
E-mail: bshin@kangwon.ac.kr

pressure node or to the anti-pressure node. With this principle, particles inside a liquid or gaseous phase can be made to move towards a specific location.

This principle can be applied in various fields, and one representative application is separation of microparticles in suspension, in a unit process. Microparticles inside suspension can be separated using a filter of physical mesh form, centrifuge, or physiochemical coagulation, but these separation methods have drawbacks; not only are these only possible in a batch type process, the filter used for the separation needs to be cleaned or replaced at specific intervals. Petersson et al. (2004) developed a device which continuously separated erythrocytes and lipids, while making blood flow through a microfluid using an ultrasonic standing wave. During the process, due to conflicting compression of erythrocytes and lipids, erythrocytes were gathered towards the pressure nodes, while lipids were aggregated towards the anti-pressure nodes. Yasuda et al. (1997) attempted to concentrate erythrocytes inside blood at the pressure nodes in a 500 kHz ultrasonic standing wave, while Zhou et al. (1998) were able to improve the detection performance of sensors by concentrating Salmonella in the suspension towards the pressure nodes in the same 500 kHz ultrasonic standing wave. Pui et al. (1995) has developed a cell harvesting system by using an ultrasonic standing wave to align and aggregate cells, and then making them precipitate by gravity.

Researches for the design of micro-chambers suitable to the generation of ultrasonic standing waves have been progressing actively. In particular, in relation to the frequency being used, Tolt and Feke (1993) have reported that the size of the ultrasonic radiation force was far larger than that of a progressive wave of the same energy density, and the radiation force was proportional to the drive frequency; a 0.3~1.5 MHz band was the optimal to use. Coakley (1997) has stated that it was desirable to use an ultrasonic wave of higher than 1 MHz to maintain high pressure, while cavitation, which is related to the formation of violently moving air bubbles, was not created. Cho et al. (2010) investigated the effects of major design parameters on the ultrasonic standing wave generation device by applying a finite elements method. They reported that acoustic pressure was mainly affected by reflector thickness, channel width, and excitation frequency, and it was effective when the channel width was determined as an integer multiple of the half wavelength. Yasuda et al. (1997) has adopted an ultrasonic standing wave generation method, by exciting an ultrasonic wave simultaneously at both ends of a half-wavelength chamber. It took 2 minutes to concentrate erythrocytes towards the pressure nodes under an acoustic radiation force of 12.8 mJ/m^3; the suspension temperature increased from 20°C to 35°C within 8 minutes of ultrasonic oscillation. Continuous ultrasonic oscillation made the suspension temperature increase, which led to both the ultrasonic wavelength and the pressure node locations changing, which ultimately resulted in impairing the concentration degree at the pressure nodes. Therefore, the wavelength needs to be maintained constant, either by installing a cooler, or by changing the frequency of the oscillating ultrasonic wave (Gröschl et al., 1998).

Haake and Dual (2002) confirmed the possibility of controlling pressure-node location through computer simulation, either by changing the excitation voltage, or phase change in the system that generates the ultrasonic standing wave via ultrasonic wave oscillation at both ends of the chamber. Cho et al. (2008) confirmed in their experiment that the pressure node location was changed by wavelength when the frequency was changed from 2 MHz to 2.5 MHz, in a chamber of width 1.5 mm. They also reported that since the surface of the reflector is always an anti-pressure node, when the frequency was increased, particles migrated towards the reflector, while when the frequency was decreased, particles moved towards the ultrasonic wave oscillator. Also, Cho (2008) introduced the notion that if the chamber width was made as a quarter wavelength, particles could be located at the reflector, by making the reflector a pressure node. This showed the possibility of improving performance of a biosensor, by pushing the target which was flowing through the microfluidic tube, towards the surface of sensor, where the antibody was immobilized to trap the target. (Kim et al., 2009). For the rapid detection for pathogenic bacteria such as *Salmonella*, various biosensors are being studied and developed (Kim et al., 2010; Kim et al., 2011). Since this kind of sensors need only small amount of sample extract which the bacteria may be existed, special care is required to prepare the sample. In large food industry or cafeteria, more efficient concentrate technology needs to be developed for the preparation of sample.

In this research, a particle's displacement characteristics in a USW field were analyzed to investigate the effects of major parameters for developing a particle separation device, and these effects were experimentally evaluated,

using the up-stream cylindrical type chamber.

Materials and Methods

Theoretical analysis for a particle movement

Particle movement equation at x-direction

If particle size is very small as compared to the ultrasonic standing wavelength λ, the ultrasonic force F_r on a particle of volume V_c which is distance x from the pressure node, as shown in Figure 1, can be calculated as in Equation (1) (Hawkes and Coakley, 2001).

$$F_r = \frac{\pi P_0^2 V_c \beta_f}{2\lambda} \varnothing(\beta,\rho) \sin\frac{4\pi x}{\lambda} \quad (1)$$

where, $0 \le x \le \frac{\lambda}{2}$

Here, P_o is the maximum acoustic pressure [Pa] and λ is the ultrasonic wavelength [m] in suspension. $\varnothing(\beta,\rho)$ is an acoustic contrast factor, and can be obtained by using Equation (2) according to the physical characteristics of particles; if the result becomes a positive number, particles move towards the pressure node, while if the resulting value becomes negative, particles move towards the anti pressure node (Johnson and Feke, 1995).

$$\varnothing(\beta,\rho) = \frac{5\rho_p - 2\rho_f}{2\rho_p - \rho_f} - \frac{\beta_p}{\beta_f} \quad (2)$$

Here, β_p and β_f are the compression degree of particles and aqueous solution, and ρ_p and ρ_f are their densities, respectively.

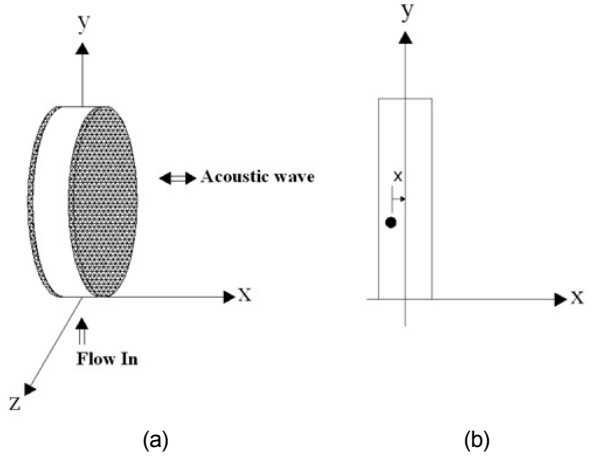

Figure 1. USW chamber, (a) schematic view and (b) a particle on the x-y plane.

Meanwhile, the drag force F_d received by particles that are pushed by ultrasonic radiation forces is obtained using Equation (3) below.

$$F_d = 6\pi\mu R\frac{dx}{dt} \quad (3)$$

Here, R and μ are the radius of particles and the dynamic viscosity of water, respectively.

Since $m_p \frac{d^2x}{dt^2} = (F_r - F_d)$, the equation of a particle's motion in the x-direction is arranged as below in Equation (4).

$$\left(\frac{4}{3}\pi R^3\rho_p\right)\frac{d^2x}{dt^2} = \frac{\pi P_0^2 V_c \beta_f}{2\lambda} \varnothing(\beta,\rho) \sin\frac{4\pi x}{\lambda} - 6\pi\mu R\frac{dx}{dt} \quad (4)$$

Particle movement equation at y-direction

When suspension in which particles are present is flowing into a chamber through its bottom, these particles undergo the flow force, F_f of suspension as in Equation (5), drag force, F_d as per Stoke's law as in Equation (6), and buoyancy, F_d as in Equation (7) in the upper direction.

$$F_f = 6\pi\mu R U_f(z) \quad (5)$$

$$F_d = 6\pi\mu R\frac{dy}{dt} \quad (6)$$

$$F_b = \frac{4}{3}\pi R_3(\rho_f - \rho_p)g \quad (7)$$

Here, $U_f(z)$ is the speed profile of suspension.

Since $m_p \frac{d^2y}{dt^2} = (F_f - F_d) + F_b$, the equation of particle motion in y-direction can be expressed as in Equation (8).

$$\left(\frac{4}{3}\pi R^3\rho_p\right)\frac{d^2y}{dt^2} = 6\pi\mu R\left(U_f(z) - \frac{dy}{dt}\right) + \frac{4}{3}\pi\mu R^3(\rho_f - \rho_{p)}g \quad (8)$$

For the investigation of more accurate particle displacement characteristics, although force between particles and van der Waals force between wall and particles should be considered (Cho et al., 2008), the purpose of this study was to find out major factors for designing the USW generating device and its drive; therefore other minute forces have been ignored.

Computer simulation

The effects of major parameters on the displacement characteristics of particles inside suspension were investigated by obtaining the value of second-order differential

Table 1. Major parameters used in the computer simulation

β_f	4.44 x 10^{-10}Pa^{-1}at25℃ (water)
β_p	2.46 x 10^{-10}Pa^{-1}at25℃ (PSlatex)
ρ_f	1,000 kg/m^3
ρ_p	1,056 kg/m^3
μ	0.001 kg/s-m
c	1,500 m/sec at 25℃ (water)

(Hawkes and Coakley, 2001; Townsend et al., 2004)

equations for both x-direction and y-direction, which were derived in the previous section using the ode45 function of MATLAB. Table 1 shows the major parameters which have been used for simulation, and the time course during which acoustic pressure P_o, particle size, and time required for particles to reach pressure node were utilized as major performance assessment factors.

For the y-direction, by considering particle size, suspension speed etc., an attempt was made to find out a minimum suspension flow speed that can move particles by its flow. In this paper, suspension speed inside the chamber should be laminar flow of low speed, thus the velocity profile in a chamber $U_f(z)$ was calculated as a simple constant.

Fabrication of ultrasonic standing wave chamber

The chamber designed for this research was prepared by cutting acrylic tube of inner diameter 32 mm to an appropriate length, and inserting PZT holders from both ends to make a hollow space at the center, the fabricated chamber being of 4.5 mm width. The PZTs were of low cost material which is used for hairdressing of diameter 25 mm, thickness 2 mm, and were fixed with silicone while being seated in the plastic holders. Holes of diameter 3 mm were made in the upper and lower portion of acrylic tube which constituted the chamber, to inject and discharge suspension into and from the chamber. Figure 2 shows an exploded view of the ultrasonic standing wave chamber, while Figure 3 shows the resonance characteristics of PZT, which were measured by impedance analyzer (HP4194A, Hewlett-Packard Japan, Ltd., Japan).

Experimental apparatus

To generate the ultrasonic wave, PZT was excited by using an RF amplifier (AG1021, T&C Power Conversion, Rochester, NY, U.S.A.). The same PZT was used as a reflector for the purpose of confirming ultrasonic standing

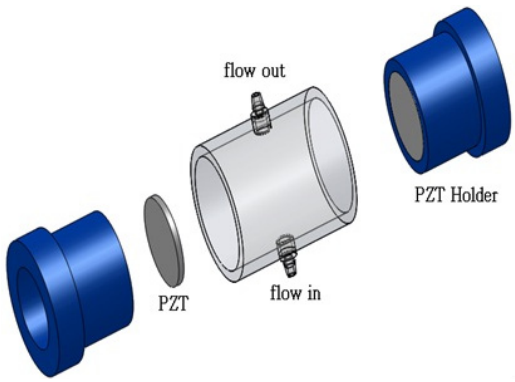

Figure 2. Exploded view of fabricated USW chamber.

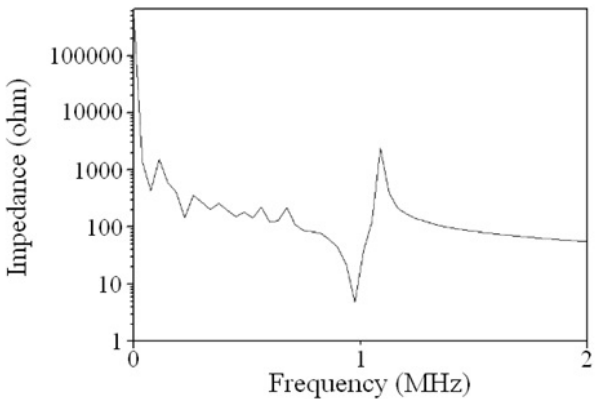

Figure 3. Impedance characteristics of PZT.

wave generation, through observing the phase difference between ultrasonic excitation signal and input signal into the reflective PZT, as well as amplitude. The output signal of the RF amplifier was branched by a T-connector, and the voltage signal that was input from the reflective PZT, were together input into an oscilloscope (TDS380, Tektronix Inc., Beaverton, OR, U.S.A.). A digital USB camera (AM413T Dino-Lite Pro, AnMo Electronic Co., Hsinchu, Taiwan) of magnification x200 was used to shoot characteristics of particle separation generated by the ultrasonic standing wave. Figure 4 shows the experimental device setup.

Particles used for the experiment were polystyrene of diameter 10 ㎛ and 100 ㎛ (Sigma-Aldrich, St.Louis, MO, U.S.A.), and the particle mass, whose amount was enough to be recognized by naked eye, was mixed into distilled water, and then made to flow into the chamber through its bottom, with the help of a syringe pump (NE-1000, New Era Pump Systems, Inc., Farmingdale, NY, U.S.A.).

Experimental method

Experiments were carried out to investigate the system

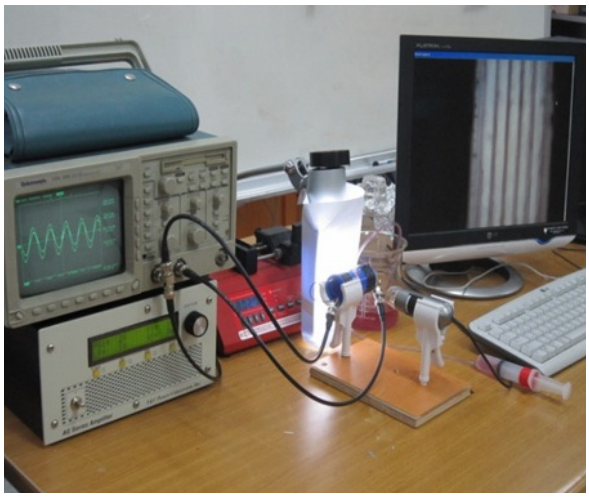

Figure 4. Experimental apparatus.

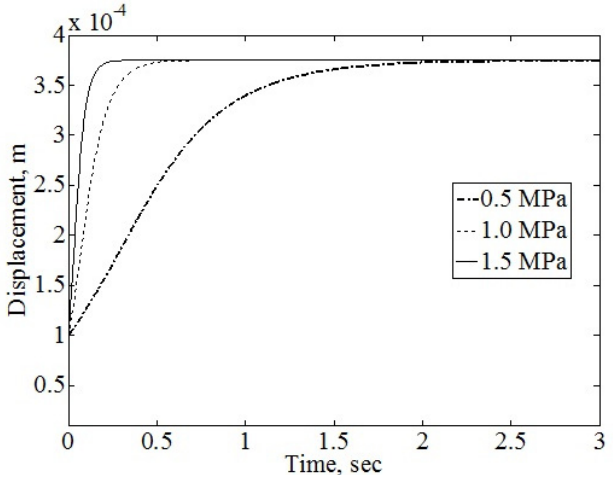

Figure 5. Displacement of a particle under different acoustic pressures with particle of 10 μm.

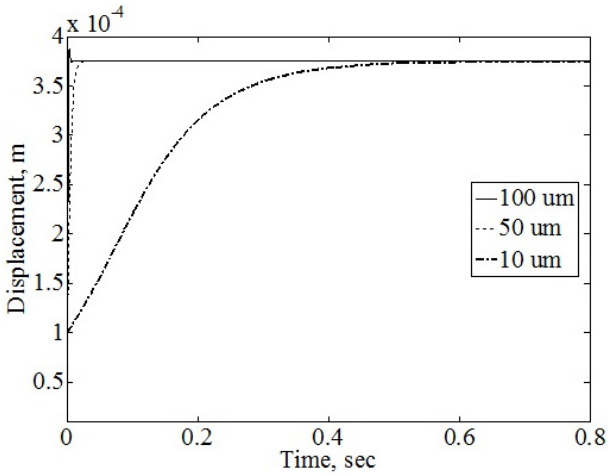

Figure 6. Displacement of a particle for different sizes at max. acoustic pressure of 1.0 MPa.

operating factors, such as resonance frequency, acoustic pressure, and flow rate, that were expected to have the largest effect on the particle separation by ultrasonic standing wave for various structural parameters such as chamber width and particle size.

First of all, the theoretically calculated pressure node locations, gap between pressure nodes, alignment of particles that were aggregated on the pressure node planes, and time required for particle alignment were measured while changing the acoustic pressure and excitation frequency inside a chamber of given width. Here, the acoustic pressure could be adjusted to the excitation voltage (V_{rms}) at the ultrasonic wave sending part, by adjusting the output of the RF amplifier. The excitation frequency was determined as that one by which the alignment of particles was well achieved, while adjusting the frequency of the RF amplifier with appropriate resolution power inside the suspension, and centered on 975 kHz which is the resonance frequency of PZT under atmospheric air, as can be seen from Figure 3.

Meanwhile, to investigate the alignment performance as per flow rate, an ultrasonic standing wave was generated to align particles at the pressure node, and then the flow rate was increased until the alignment plane was broken, thus the flow rate at breaking point was regarded as the maximum flow rate.

Alignment characteristic inside the chamber was analyzed from image shoot at 0.1 sec intervals.

Results and discussion

Theoretical analysis

As in Equation (1), a pressure node appeared for the first time at the point distant from the reflector (x=0) by as much as λ/4. Theoretically, the particle that started from the point where x was a little bit larger than 0, would reach 0.375×10^{-3} m. Figures 5 and 6 represent the trajectory of particle movement in the x-direction when either acoustic pressure or particle size are changed, indicating that this trajectory accurately reaches its target value. As acoustic pressure increased, movement speed of a particle became faster. The larger the particle size, the faster it reached the pressure-node. This is because when both the acoustic pressure and particle size increase, the radiation force of

Table 2. Elapsed time to reach the adjacent pressure node plane

		Diameter of a particle(μm)		
		100	50	10
P_o (MPa)	0.5	0.025 s	0.09 s	2.48 s
	1.0	*0.009 s	0.023 s	0.58 s
	1.5	*0.005 s	0.009 s	0.27 s

* overshoot observed

the ultrasonic standing wave also increases. Table 2 indicates the time requirement of a particle reaching its target value while the size of acoustic pressure and of the particles were changed.

Since the displacement characteristics of a particle in the y-direction is only a function of the size of particle and the suspension ascending speed by the inlet flow rate of suspension, computer simulation was carried out to search the critical speed of up-streaming suspension for a given particle size. Based on trial and error, the particle was considered to be levitated in a suspension when it was moving up and down only within a range of $\pm 6 \times 10^{-10}$ m of the current location. The critical speeds of up-stream were found to be 3.069×10^{-4} m/s, 0.76×10^{-4} m/s, and 0.038×10^{-4} m/s for a corresponding particle size of 100 ㎛, 50 ㎛ and 10 ㎛ respectively. When flow rate is higher than the critical level, particles ascend by the flow of fluid; but if the flow rate is less than the critical level, particles precipitate by gravity, which exercises a stronger effect than other factors. It is therefore judged that critical flow velocity can be increased in proportion to the square of particle diameter, and that the particles are being transported while maintaining their alignment, provided that the suspension that is supplied is at least enough to maintain a higher than minimum critical flow velocity.

Particle separation by ultrasonic standing wave

Theoretically, the first pressure node appears at the location distant from the reflector by as much as $\lambda/4$, and then again reappears at every $\lambda/2$ interval. Since the width of chamber which determines the distance between the sending and receiving part of the ultrasonic wave should be an integer multiple of $\lambda/2$, the last pressure node would maintain a gap of $\lambda/4$ from the ultrasonic wave transmission part. When the excitation frequency is 1 MHz, the ultrasonic wave transmission speed inside suspension is assumed to be 1,500 m/s, the wavelength becomes 1.5 mm and if the chamber width is maintained as 4.5 mm, this is equivalent to 3 λ, thus a total of 6 bands of pressure node planes should be formed.

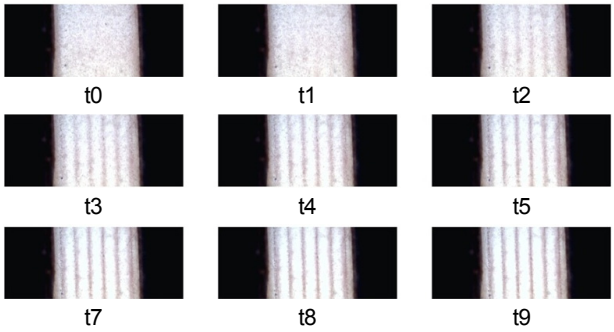

Figure 7. Alignment of particles on pressure-node planes with the lapse of time.

Figure 7 shows particles of size 10 ㎛ are being aligned at pressure-nodes with time elapse by generating an ultrasonic standing wave at a PZT excitation voltage of 12.5 V and excitation frequency of 980 kHz. Under these conditions, the wavelength of ultrasound is around 1.51 mm, and the pressure node should appear at 0.0397 mm from the reflector; after that the 2nd~6th pressure nodes should appear at every 0.758 mm interval. Since the focus of camera was adjusted to the center of the chamber, it was difficult to measure the distance by distinguishing the chamber wall; yet it could be confirmed that the pressure nodes at which particles were aligned were of uniform gap. Since the phases of excitation signal and the signal that came out from the reflector PZT were observed at the same phase, it could be confirmed as well that the ultrasonic standing wave was normally generated.

Effect of excitation voltage

Figure 8 shows the observation result of particle alignment while changing the excitation voltage imposed on the PZT in order to change acoustic pressure, where a particle size of 10 ㎛ was used, and the excitation frequency was 980 kHz. The images were taken at 0.3 sec. elapsed time after starting the ultrasonic wave trans-

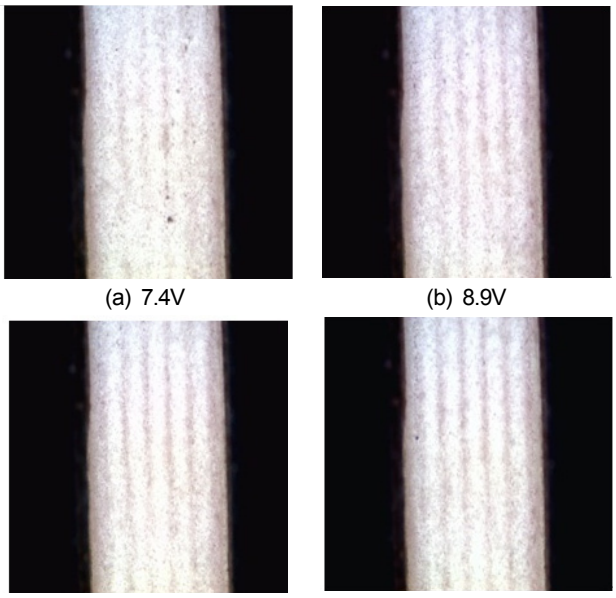

Figure 8. Alignment of particles for different excitation voltages at t = 0.3 sec.

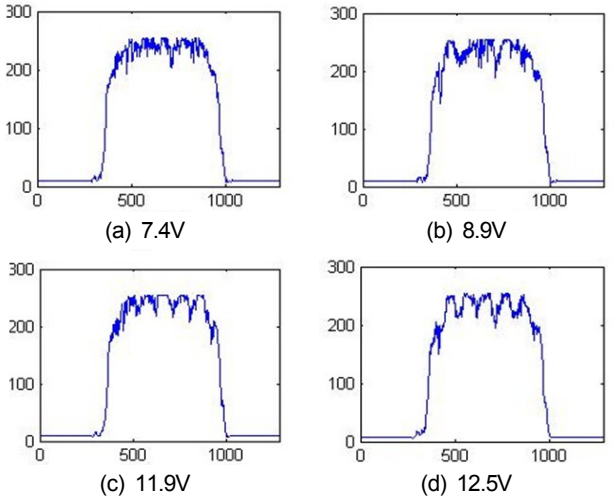

Figure 9. Comparison of particle alignment by pixel intensity on a horizontal line across the chamber (x-axis : Pixel no. across the chamber width, y-axis : Light intensity (0-255)).

mission. It can be seen from comparison of the images that alignment of the particles becomes clear with increases in voltage level. As has been reviewed in the computer simulation, this was in confirmation with the results of particle transport speed towards pressure-nodes when the acoustic pressure was increased, i.e. the excitation voltage was increased.

For a clearer comparison, the brightness of pixels was examined across the chamber width for the horizontal line at center of the image. As shown in Figure 9, the dark peaks

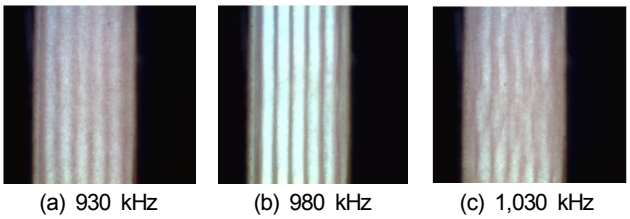

Figure 10. Alignment of particle for different PZT driving frequencies.

(particle band) became clearer as the excitation voltage increased. It can be confirmed that with increase in excitation voltage, particles align, resulting in a clear distinction between bands of particle alignment with less brightness, and other zones with easy light penetration.

Effect of driving frequency

The effects of frequency variation on the particle alignment characteristics were investigated at a fixed chamber width of 4.5 mm by changing the excitation frequency from 920 kHz to 1,040 kHz. Figure 10 shows typical images taken at the time of 2 sec after transmission of the ultrasonic wave, when the alignment was completed, over interested frequencies. From the figure, it is clear that particles were aligned at the pressure-node at an excitation frequency within ± 50 kHz from the center frequency of 980 kHz, but when the frequency was increased higher than the critical level, alignment became dispersed, and with further increase or decrease of frequency, particle alignment was no longer evident. If the velocity of ultrasonic wave in water is considered as 1,490 m/sec under a room temperature of around 20°C, the wavelength would be 1.52 mm at a frequency of 980 kHz, while the wavelengths would change to 1.60 mm and 1.45 mm at frequencies of 930 kHz and 1,030 kHz, respectively. Therefore, the required space (3λ) for forming 6 bands of pressure-nodes should be 4.62 mm, 4.80 mm and 4.33 mm at frequencies of 980 kHz, 930 kHz and 1,030 kHz, respectively. However, since in this research the chamber width is 4.5 mm, although 6 bands of pressure-node planes can form within ± 0.3 mm, above that level an ultrasonic standing wave has not been able to be generated, because the wavelength and chamber width do not match.

Effect of particle size

The effect of particle size on alignment characteristics was evaluated using particles of 100 ㎛ and 10 ㎛ in solution, at an excitation voltage of 10.0 V and frequency of

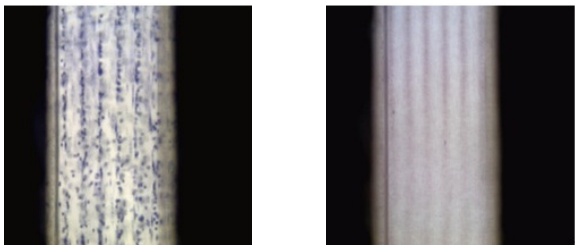

(a) 100 μm (b) 10 μm

Figure 11. Effect of particle size on alignment characteristics.

Table 3. Maximum inlet flow rate for maintaining particle alignment at different excitation voltages

Excitation voltage(V)	Flow rate(ml/min)
5.2	7.4
7.5	9.9
9.4	11.9
10.5	15.8

980 kHz. In separate experiments, solutions of two sizes of particle were injected into the chamber, and the particle alignment process was observed. The images at the time the alignment was established are shown in Figure 11. Through image analysis taken every 0.1 sec, the particles of 100 ㎛ in diameter lined up within 0.1 sec, while alignment was observed for the particles of 10 ㎛ at 0.9 sec. This phenomenon indicated that the larger the particle size, the faster was its movement towards the pressure-node plane.

Effect of inlet flow rate

Table 3 shows the maximum inlet flow rate into a chamber for which the particle alignment plane was not broken during upward transportation by possible disturbance due to fast flow of upstream when the flow rate of suspension was increased. Under the given conditions of operation at an excitation frequency of 980 kHz with particle size 10 ㎛, a greater inlet flow-rate was allowable as the excitation voltage increased. The higher excitation voltage generated more radiation force with which to trap particles in a certain boundary of the pressure-node plane. Above the maximum flow rate, the force exerted on the particles by the flow itself became larger than the trapping force, which resulted in breaking the particle alignment on the pressure-node plane. Therefore, it was concluded that the maximum flow rate could be obtained experimentally under a given excitation voltage, after fabrication of a chamber for particle separation. This flow rate would be the maximum throughput to make particle separation possible inside the given chamber.

Conclusions

The effects of excitation voltage and flow rate in a solution, which are major designing parameters for the particle separation device, were investigated through computer simulation by establishing a mathematical model for the displacement characteristics of particles which are exposed to an ultrasonic standing wave field. The results of theoretical analysis were experimentally validated with a cylindrical type chamber, and at the same time the effects of major operational parameters on the particle separation characteristics of the system were investigated. Major research findings are summarized as follows:

(1) A total of 6 bands of acoustic pressure-node planes were confirmed by naked eye as well as by photograph image, under the conditions of chamber width of 4.5 mm, and an excitation frequency of 980 kHz, which was the same as that obtained for PZT by theoretical analysis.
(2) With increase in excitation voltage and particle size, particles received a larger acoustic pressure and thus moved more rapidly towards an acoustic pressure-node plane.
(3) As regards excitation frequency tolerance, 6 bands of pressure-node planes were formed at the frequency range of 980 ± 50 kHz, but as the excitation frequency varies further from the center frequency of 980 kHz, the distribution of particles that have been aligned at pressure-node planes becomes wider, and ultimately an ultrasonic standing wave field cannot be formed beyond the frequency range.
(4) The maximum inlet flow rate can be determined when the particles in a solution are being transported upward while maintaining particle alignment at the pressure-node planes. A higher excitation voltage allows a greater inlet flow rate of suspension into the chamber.

Conflict of Interest

No potential conflict of interest to this article was reported.

Acknowledgements

This study was supported by Kangwon National University.

References

Cho, S. H. 2008. Particle separation and control technology using ultrasound. Noise & Vibration 18(5):14-19 (In Korean, with English abstract).

Cho, S. H., D. -C. Seo, B. Ahn, K. -B. Kim and Y. -L. Kim. 2008. Position control of micro particles in a fluid flow using ultrasonic standing wave. Journal of Korean Society for Nondestructive Testing 28(2):131-136 (In Korean, with English abstract).

Cho, S. H., J. H. Park, B. Ahn and K.-B. Kim. 2010. Finite Element Analysis of a Particle Manipulation System Using Ultrasonic Standing Wave. Journal of KSNVE 20(1):3-9 (In Korean, with English abstract).

Coakley W. T. 1997. Ultrasonic separations in analytical biotechnology. Trends in Biotechnology 15:506-511.

Gröschl M., W. Burger and B. Handl. 1998. Ultrasonic separation of suspended particles - Part III: Application in Biotechnology. ACUSTICA•acta acustica 84:815-822.

Haake, A and J. Dual. 2002. Micro-manipulation of small particles by node position control of an ultrasonic standing wave. Ultrasonics 40:317-322.

Hawkes, J.J. and W.T. Coakley. 2001. Force field particle filter, combining ultrasound standing waves and laminar flow. Sensors and Actuators B 75:213-222.

Johnson, D.A. and D.L. Feke. 1995. Methodology for fractionating suspended particles using ultrasonic standing wave and divided flow fields. Separation Technology 5:251-258.

Kim, E. H., H. K. Cho, K.S. Kyung and G. Kim. 2009. Detection of the Fungicide Iprovalicarb Residues Using a Surface Plasmon Resonance Biosensor. Journal of Biosystems Engineering 34(1):50-56 (In Korean, with English abstract).

Kim, G., G. M. Yang, Y. H. Kim, C. Y. Mo and S. B. Park. 2010. Detection of pathogenic Salmonella with a composite quantum dot. Journal of Biosystems Engineering 35 (6):458-463 (In Korean, with English abstract).

Kim, G., G. Yang, S. B. Park, Y. H. Kim, K. J. Lee, J. Y. Son, H. J. Kim and S. R. Lee. 2011. Rapid detection kit for Salmonella typhimurium. Journal of Biosystems Engineering 36(2):140-146 (In Korean, with English abstract).

Laurell, T., F. Petersson and A. Nilsson. 2007. Chip integrated strategies for acoustic separation and manipulation of cells and particles. Chem. Soc. Rev. 36: 492-506.

Petersson, F., A. Nilsson, C. Holm, H. Jonsson and T. Laurell. 2004. Separation of lipids from blood utilizing ultrasonic standing waves in microfluidic channels. Analyst 129:938-943.

Pui, P.W.S., F. Trampler, S.A. Sonderhoff, M. Groschl, D.G. Kilburn and J.M. Piret. 1995. Batch and Semicontinuous Aggregation and Sedimentation of Hybridoma Cells by Acoustic Resonance Fields. Biotechnol. Prog. 11: 146-152.

Tolt T. L. and D. L. Feke. 1993. Separation of dispersed phases from liquids in acoustically driven chambers. Chemical Engineering Science 48(3):527-540.

Townsend R.J., M. Hill, N.R. Harris and N.M. White. 2004. Modelling of particle paths passing through an ultrasonic standing wave. Ultrasonics 42:319-324.

Yasuda K., S. S. Haupt, S. Umemura, T. Yagi, M. Nishida and Y. Shibata. 1997. Using acoustic radiation force as a concentration method for erythrocytes. J. Acoust. Soc. Am. 102(1):642-645.

Zhou C., P. Pivarnik, A. G. Rand and S. V. Letcher. 1998. Acoustic standing-wave enhancement of a fiber-optic Salmonella biosensor. Biosensors & Bioelectronics 13: 495-500.